Estimation of Sea and Lake Ice Characteristics with GOES-R ABI

Xuanji Wang[1], Jeffrey R. Key[2], Yinghui Liu[1], William Straka III[1]
[1]Cooperative Institute for Meteorological Satellite Studies (CIMSS) / Space Science and Engineering Center (SSEC), UW-Madison, Madison, Wisconsin
[2]Center for Satellite Applications and Research, NOAA/NESDIS, Madison, Wisconsin

Introduction

The cryosphere exists at all latitudes and in about one hundred countries (Fig.1). It has profound socio-economic value due to its role in water resources and its impact on transportation, fisheries, hunting, herding, and agriculture. The cryosphere not only plays a significant role in climate; its characterization and distribution are critical for accurate weather forecasts. A number of ice characterization algorithms have been improved and/or developed for the next generation Geostationary Operational Environmental Satellite (GOES-R) Advanced Baseline Imager (ABI), including ice identification and concentration, ice extent, ice thickness and age, and ice motion. An overview of the ice characterization algorithms will be provided and their preliminary results will be shown here with applications to SEVIRI, AVHRR, and MODIS data.

Current operational GOES imager algorithms utilize heritage channels from both the Advanced Very High Resolution Radiometer (AVHRR) and the Moderate Resolution Imaging Spectroradiometer (MODIS) for the estimation of sea and lake ice characteristics. Mature algorithms exist for ice identification and ice surface temperature, but others such as ice concentration, ice thickness and age, and ice motion are experimental or under development. Errors in existing algorithms must be determined by inter-comparing products from other sensors and comparing those products to surface-based observations. Potential solutions to problems have been sought and new algorithms for estimating ice concentration, ice thickness/age, and ice motion have been developed as necessary. This work will serve as a testbed of the current and developing algorithms for sea and lake ice products. Preliminary tests are promising, and we expect that accuracy specifications will be met for most of the cryosphere products in the 2009-2010 timeframe.

Global Cryosphere by Type

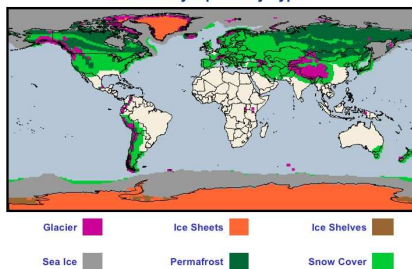Glacier Ice Sheets Ice Shelves
Sea Ice Permafrost Snow Cover

Fig. 1. The global distribution of the Cryosphere by type.

Sea and Lake Ice Concentration and Extent

Sea ice is detected through the use of a grouped threshold technique. A pixel is identified as sea ice when it has a normalized difference snow index $(NDSI = (R0.55-R1.64)/(R0.55+R1.64))$ greater than 0.4, a visible reflectance at 0.865 μm greater than 0.11, and a visible reflectance at 0.645 μm greater than 0.10 (Fig.2). For ice/snow surface temperature (IST) retrieval from the AVHRR and MODIS we use the equation

$$T_s = a + bT_{11} + c(T_{11} - T_{12}) + d[(T_{11} - T_{12})(\sec\theta - 1)]$$

where T_s is the estimated surface temperature (K), T_{11} and T_{12} are the brightness temperatures (K) at 11 μm (AVHRR channel 4, MODIS band 31) and 12 μm (AVHRR channel 5, MODIS band 32) and q is the sensor scan angle. Coefficients a, b, c, and d are derived for the following temperature ranges: $T_{11} < 240K$, $240K < T_{11} < 260K$, $T_{11} > 260K$. This has been adapted to SEVERI. Ice concentration is derived via a tie point analysis. A local search window is used to derive ice and water tie points (Fig.3), with additional synoptic corrections on the ice tie point. Ice extent is determined based on ice concentration. During the day, both visible reflectance and calculated ice surface temperature (IST) are used to derive ice concentration, while only IST is used during nighttime. Preliminary results are shown in Fig.4 and 5.
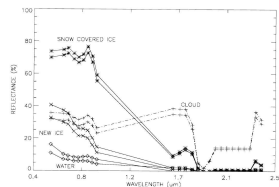

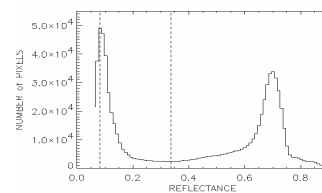**Fig. 2.** Reflectance means for samples of ice, clouds, and water (Riggs et al. 1999).

Fig. 3. Distribution of 640 nm reflectance for an ice/water scene. The ice/water threshold reflectance (0.336) and the water tie point (0.083) are indicated. (Appel and Jensen, Fresh water ice VIIRS ATBD, 2002)
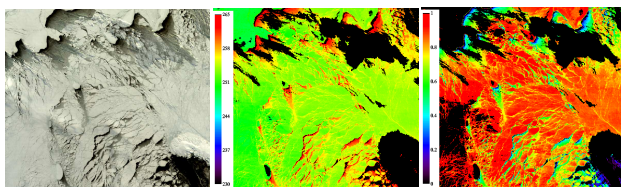

Fig. 4. MODIS Aqua true color image (left) on March 31, 2006 over Kara Sea, and derived surface skin temperature in Kelvin degree (middle), and ice concentration in percentage (right).
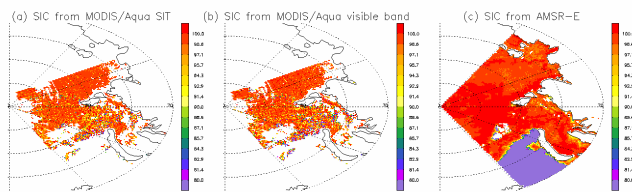

(a) SIC from MODIS/Aqua SIT   (b) SIC from MODIS/Aqua visible band   (c) SIC from AMSR−E

Fig. 5. Sea ice concentration (SIC) (%) retrieved from (a) MODIS Sea Ice Temperature (SIT), (b) MODIS visible band reflectance, and (c) from Advanced Microwave Scanning Radiometer - Earth Observing System (AMSR-E) Level-3 gridded daily mean from NSIDC on March 31, 2006. MODIS retrievals compare well with AMSR-E retrievals, and show more detailed information.

Sea and Lake Ice Thickness and Age

A One-dimensional Thermodynamic Ice Model (OTIM) was created based on the surface energy balance at thermo-equilibrium that contains all components of the surface energy balance to estimate sea/lake ice thickness. The equation for energy conservation at the top surface (ice or snow) is

$$(1-\alpha_s) F_r - I_0 - F_{up} + F_{dn} + F_s + F_e + F_c = 0$$

where α_s is surface ice/snow broadband albedo, F_r is surface downward solar radiation, I_0 is the solar radiation passing through the ice interior, F_{up} and F_{dn} are surface upward and downward longwave radiations, respectively. F_s, F_e, and F_c are surface turbulent sensible, latent, and conductive heat fluxes, respectively. Based on the ice thickness, seven categories of ice "age" are defined: new ice (0.00~0.10 m), grey ice (0.10~0.15 m), grey-white ice (0.15~0.30 m), thin first-year ice (0.30~0.70 m), medium first-year ice (0.70~1.00 m), thick first-year ice (1.00~1.50 m), and old ice including second-year and multi-year ice (> 1.50 m). The thicker categories are for sea ice only. The current version of the OTIM was compared with the ice draft data measured by submarine upward looking sonar during the Scientific Ice Expedition (SCICEX) in 1999, and also compared with the simulated ice thickness data from Pan-Arctic Ice-Ocean Modeling and Assimilation System (PIOMAS) (Fig.6). Preliminary results are shown in Fig. 7 and 8.
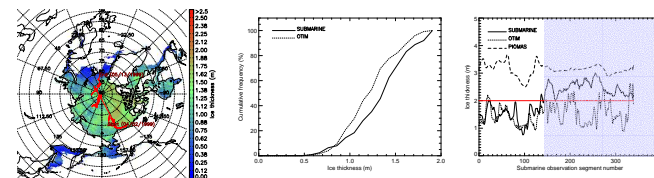

Fig. 6. The submarine track during the SCICEX experiment in 1999 with starting and ending dates marked on the plot (left), the comparison of ice thickness cumulative frequency distribution from OTIM and submarine sonar (ice draft, middle), and a point-to -point comparison of the ice thickness from OTIM, PIOMAS, and submarine (right) during that period along the submarine track. OTIM ice thickness products were produced with AVHRR data. Overall, OTIM performs well when actual ice thickness is less than 2 meters. PIOMAS always overestimates ice thickness compared to the submarine ice draft data.
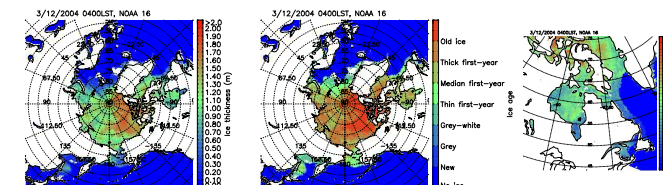

Fig. 7. OTIM retrieved ice thickness (left) and ice age (middle) based on AVHRR data on March 12, 2004 at 04:00 LST for the entire Arctic region and Hudson Bay area ice thickness (right).
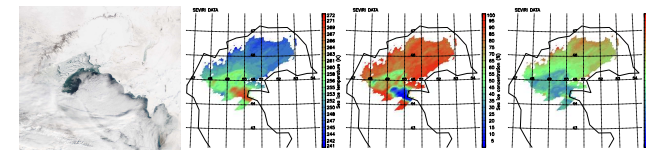

Fig. 8. MODIS true color image over the Caspian Sea on January 27, 2006 and the corresponding ice surface temperature, sea ice concentration, and sea ice thickness.

Sea Ice Motion

An algorithm developed by C. Fowler, J. Emery, and J. Maslanik (IEEE Geoscience and Remote Sensing Letters,Vol.1, No. 2, pp.71-74, April 2004) was adopted in this study. It is basically a statistical method; maximum-cross correlation (MCC) is employed for ice motion calculations. Fig. 9 gives an example over the Arctic based on MODIS data.
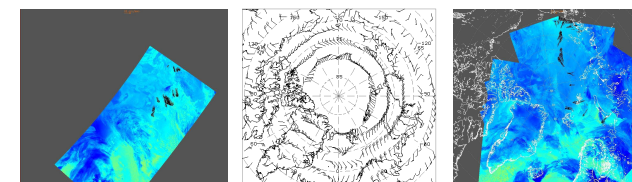

Fig. 9. Comparison of ice motion from MODIS, utilizing the Tromsø direct broadcast site for 1252 UTC on 3 Nov, 2007, and the MRF model surface winds (middle) at 12 UTC. Orientation is the same on both images (left and middle). A composite for Dec. 19, 2007 is shown on the right.